Available online at www.sciencedirect.com
ScienceDirect
Polymer 49 (2008) 1455–1466
polymer
www.elsevier.com/locate/polymer

Optically active 2,4-dimethylglutarate azoaromatic esters of known relative configuration as models of dyads present in the related methacrylic polymeric derivatives

L. Angiolini*, T. Benelli, L. Giorgini, E. Salatelli, T. Zuccheri

Dipartimento di Chimica Industriale e dei Materiali and INSTM UdR-Bologna, University of Bologna, Viale Risorgimento 4, 40136 Bologna, Italy

Received 8 December 2007; received in revised form 28 January 2008; accepted 5 February 2008
Available online 8 February 2008

Abstract

Novel chiral dimeric models of *isotactic* (*meso*) and *syndiotactic* (*dl*) dyads of optically active methacrylic polymers containing in the side-chain the pyrrolidinyl group of one single configuration linked through the nitrogen atom to the azobenzene chromophore, have been synthesized by functionalization of 2,4-dimethylglutaric acids with known streoisomeric composition.

Their characterization afforded the possibility to investigate the relationship between the chiroptical and spectroscopic properties displayed by the dimeric model compounds and those of the related homopolymeric derivatives with known main chain stereoregularity.

In particular, the optical rotation values and circular dichroism spectra of the models allow to establish the contribution of main chain micro-tacticity to the overall optical activity of the polymeric derivative.

Keywords: Chiroptical properties; Side-chain azobenzene polymers; Chiral amplification

1. Introduction

An intense attention has currently arised to investigations dealing with chiral nanotechnology [1,2] and the amplification of chirality in polymeric materials [3–6].

Since the 1980s, Mario Farina undertook a deep study of polymer stereochemistry and its effect on chain conformation [7]. More recently in literature have been reported several examples of polyisocyanates whose chains can be induced to take an helical conformation with a prevailing screw sense, by incorporation of small enantiomeric excesses of chiral pendant groups in the side chain [8,9] or by photoresolution [10]. Polyisocyanates functionalized with chiral azoaromatic dyes as side chain resulted capable of a reversible shift of the preferred helical twist sense by photochemical isomerization of the chromophores [11].

Optically active photochromic polymers bearing in the side chain both a chiral group of one single configuration and the *trans*-azoaromatic moiety with a conjugated electron donor–acceptor system, have received considerable attention for their potential in advanced technological applications, also. Displaying, in fact, both the properties typical of dissymmetric systems [12] (optical activity, absorption of circularly polarized light in the UV–vis spectral region), as well as the features of photochromic materials [13–15] (NLO properties, photoresponsiveness, photorefractivity), they can be proposed as devices [16–20] for optical data storage, holographic memories, waveguides, chemical photoreceptors, etc.

We have recently observed [21–23] that it is possible to photomodulate the chiroptical properties of thin films of chiral photochromic polymethacrylates by irradiation with circularly polarized light of one single *L* or *R* rotation sense. This unexpected new phenomenon seems to open new possibilities for the use of azobenzene containing materials as chiroptical switches, besides the usual applications in optics. The synthesis and characterization of polymethacrylates bearing a rigid

* Corresponding author. Tel./fax: +39 051 2093687.
E-mail address: luigi.angiolini@unibo.it (L. Angiolini).

0032-3861/$ - see front matter © 2008 Elsevier Ltd. All rights reserved.
doi:10.1016/j.polymer.2008.02.008

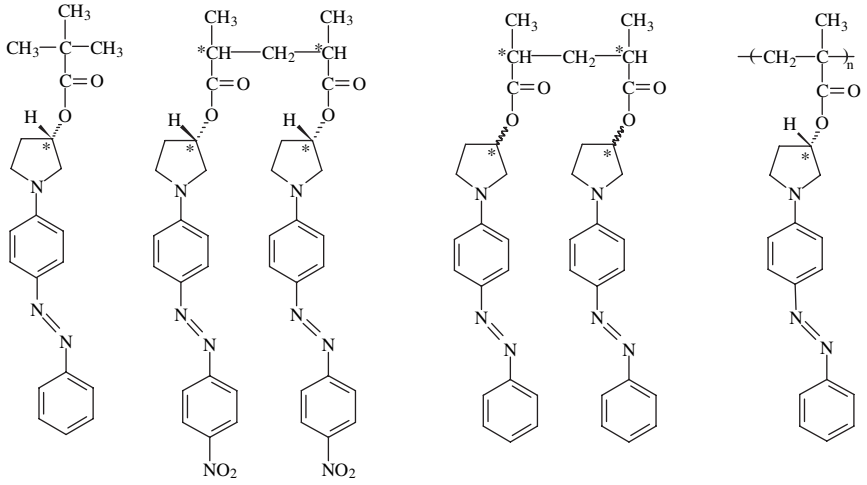

(*S*)-**PAP** Dim[(*S*)-**DMGAP-N**]-(32.2% *meso*) Dim[(*S*)-**DMGAP**]-(71.0% *meso*) Dim[(*S*)-**DMGAP**]-(40.9% *meso*) Dim[(*S*)-**DMGAP**]-(0% *meso*) Dim[(*R*)-**DMGAP**]-(67.6% *meso*) Poly[(*S*)-**MAP**]

Fig. 1. Chemical structures of model compound (*S*)-**PAP**, 2,4-dimethylglutaric dimeric models and the related homopolymer poly[(*S*)-**MAP**].

chiral group of one single configuration interposed between the main chain and the *trans*-azoaromatic chromophore has been previously reported [24,25]. The presence of conformational dissymmetry in these systems can be detected by chiroptical techniques, such as circular dichroism (CD), suitable to reveal the existence of chiral perturbation induced by the optically active moieties onto the electronic transitions of the achiral azoaromatic chromophore. Chiral interactions among side-groups, in fact, are responsible for the appearance of an ordered arrangement of the chromophores, with formation of helical structures of one prevailing screw sense, as demonstrated by strong CD exciton-couplets observed, both in solution and in the solid state, in the absorption region of the azoaromatic chromophore.

A remarkable contribution of the macromolecular structure to optical activity could be due, in principle, to conformational and/or configurational effects originated by a prevalent tacticity of the polymeric main chain. To this regard, we have recently synthesized by ATRP [26] a series of optically active methacrylic linear homopolymers such as poly[(*S*)-3-methacryloyloxy-1-(4-azobenzene)pyrrolidine] {poly[(*S*)-**MAP**]} (Fig. 1), the related star shaped polymers of C_3 symmetry [27] with different average polymerization degree (in the range 10–30), and a series of oligomeric models, such as dimer, trimer and tetramer [28]. The results suggest that even few adjacent chiral units are able to produce a remarkable conformational dissymmetry in the macromolecules, strongly dependent on their average chain length.

In addition, a recent study [29] disclosed that bis{(*S*)-(−)-3-[1-(4′-nitro-4-azobenzene)]pyrrolidine}-2,4-dimethylglutarate, shown in Fig. 1, containing the 32.2% molar amount of *meso* form of the 2,4-dimethylglutarate residue {Dim[(*S*)-**DMGAP-N**]-(32.2% *meso*)} [29], corresponding to the smallest section of polymer where interchromophore interactions can be present, is characterized by a strong CD exciton couplet of intensity about one third of that displayed by the corresponding polymer. The stereoisomeric composition of Dim[(*S*)-**DMGAP-N**]-(32.2% *meso*) is by chance similar to the main chain tacticity usually obtained for the polymeric derivative poly[(*S*)-**MAP**] prepared by radical polymerization (about 30% of *isotactic* dyads) [24–28,30–32]. Indeed, the *meso* and the *dl* stereoisomers of the 2,4-dimethylglutarate moiety can be considered as the structural models for the *isotactic* and *syndiotactic* dyads of the related methacrylic polymer, respectively (Fig. 2).

With the aim to confirm that the optical activity of such polymeric derivatives is essentially ascribed to conformational arrangement, we retained the interest to evaluate the effects of the main chain tacticity on their chirooptical properties, by investigating well-defined configurational models. Thus, we report in the present paper the synthesis and full characterization of several diesters of 2,4-dimethylglutaric acid, as dimeric models of one repeating dyad of the methacrylic homopolymer poly[(*S*)-**MAP**], that have been obtained starting from diastereomeric mixtures of different composition of

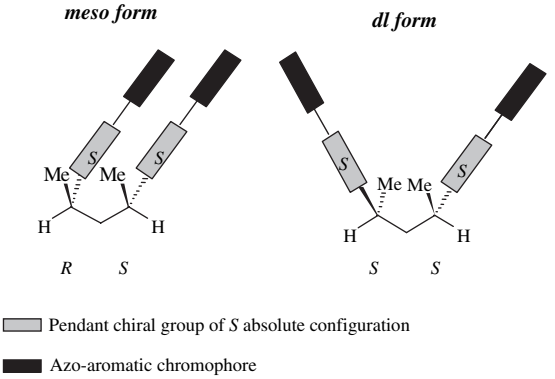

Fig. 2. Idealised representation of the *meso* and *dl* forms of the 2,4-dimethylglutaric derivatives investigated as models of *isotactic* and *syndiotactic* dyads, respectively, of the related polymethacrylate derivatives (only one stereoisomeric enantiomer is presented here).

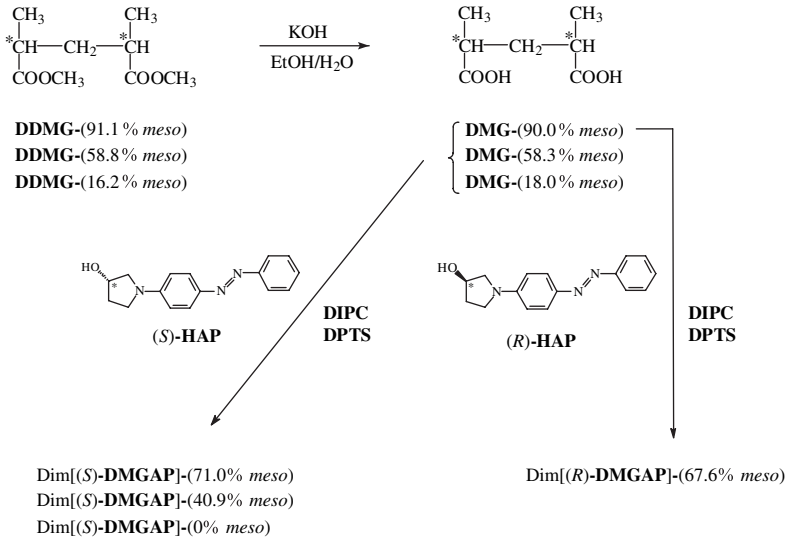

Scheme 1.

dimethyl-2,4-dimethylglutarate (**DDMG**) by reaction with the (*S*)- or the (*R*)-enantiomer of 3-hydroxy-1-(4-azobenzene)pyrrolidine [(*S*)- or (*R*)-**HAP**] (Scheme 1). The prepared models, namely bis{(*S*)-(−)-3-[1-(4-azobenzene)]-pyrrolidine}-2,4-dimethylglutarate at 71.0% and 40.9% of *meso* form, {Dim[(*S*)-**DMGAP**]-(71.0% *meso*) and Dim[(*S*)-**DMGAP**]-(40.9% *meso*), respectively}, bis{(*S*)-(−)-3-[1-(4-azobenzene)]pyrrolidine}-2,4-dimethylglutarate at 100% of *dl* form {Dim[(*S*)-**DMGAP**]-(0% *meso*)} and bis{(*R*)-(+)-3-[1-(4-azobenzene)]pyrrolidine}-2,4-dimethylglutarate at 67.6% of *meso* form of the 2,4-dimethyglutarate residue {Dim[(*R*)-**DMGAP**]-(67.6% *meso*)} are reported in Fig. 1. Models Dim[(*S*)-**DMGAP**]-(71.0% *meso*), Dim[(*S*)-**DMGAP**]-(40.9% *meso*) and Dim[(*S*)-**DMGAP**]-(0% *meso*) have been finally resolved by HPLC to give the pure stereoisomers bis{(*S*)-(−)-3-[1-(4-azobenzene)]pyrrolidine}-(*SR*/*RS*)-2,4-dimethylglutarate {(*SR*/*RS*)-Dim[(*S*)-**DMGAP**]-(100% *meso*)}, bis{(*S*)-(−)-3-[1-(4-azobenzene)]pyrrolidine}-(*SS*)-2,4-dimethylglutarate {(*SS*)-Dim[(*S*)-**DMGAP**]-(0% *meso*)} and bis{(*S*)-(−)-3-[1-(4-azobenzene)]pyrrolidine}-(*RR*)-2,4-dimethylglutarate {(*RR*)-Dim[(*S*)-**DMGAP**]-(0% *meso*)}, labelled as **a**, **b** and **c**, respectively, in Fig. 3.

Electronic spectra, optical activity and chiroptical properties of the above products have been compared with those displayed by the homopolymer poly[(*S*)-**MAP**] with a content of *syndiotactic* dyads of about 74% [24], as well as by the low molecular weight model compound (*S*)-(+)-3-pivaloyloxy-1-(4-azobenzene)pyrrolidine [(*S*)-**PAP**] [24] (Fig. 1), representative of one single optically active repeating unit of the polymeric derivative.

2. Experimental

2.1. Physico-chemical measurements

^{1}H and ^{13}C NMR spectra were obtained at room temperature, on 5−10% $CDCl_3$ solutions, using a Varian NMR Gemini 300 spectrometer. Chemical shifts are given in ppm from tetramethylsilane (TMS) as the internal reference. ^{1}H NMR spectra were run at 300 MHz by using the following experimental conditions: 24,000 data points, 4.5-kHz spectral width, 2.6-s acquisition time, 128 transients. ^{13}C NMR spectra were recorded at 75.5 MHz, under full proton decoupling, by using

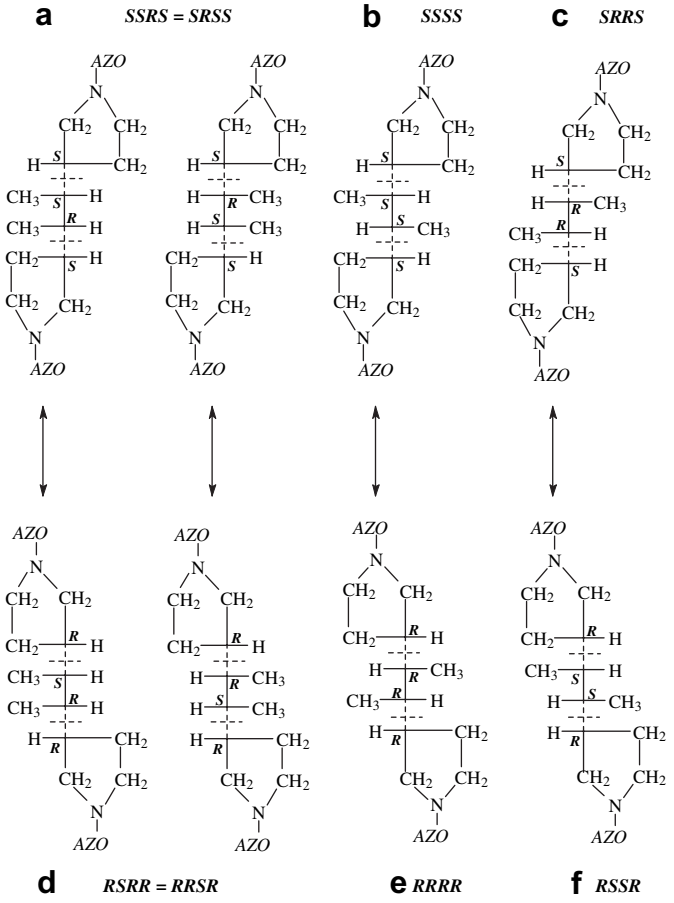

Fig. 3. Modified Fischer's illustration of the structures of the investigated dimers: **a**–**d**, **b**–**e** and **c**–**f** are optical antipodes.

the following experimental conditions: 24,000 data points, 20-kHz spectral width, 0.6-s acquisition time, 4000 transients.

The X-ray diffraction spectra were carried out at room temperature on a Bruker APEXII diffractometer equipped with a CCD detector. Intensity data were corrected for Lorentz and polarization effects. The absolute configuration of the asymmetric carbons of the DMG residues was solved on the basis of the known *S* absolute configuration of pyrrolidine moieties in the side chain.

FT-IR spectra were carried out on a Perkin–Elmer 1750 spectrophotometer, equipped with an Epson Endeavour II data station, on sample prepared as KBr pellets.

Checking of the liquid crystalline behaviour was carried out with an Zeiss Axioscope2 polarising microscope through crossed polarizers fitted with a Linkam THMS 600 hot stage.

Melting points (uncorrected) were determined in glass capillaries on a Büchi 510 apparatus at a heating rate of 1 °C/min.

UV–vis absorption spectra were recorded at 25 °C in the 700–250 nm spectral region with a Perkin–Elmer Lambda 19 spectrophotometer on $CHCl_3$ solutions by using cell path lengths of 0.1 cm and concentrations in azobenzene chromophore of about 3×10^{-4} mol L^{-1}.

Optical activity measurements were accomplished at 25 °C on $CHCl_3$ solutions ($c \approx 0.250$ g dL^{-1}) with a Perkin Elmer 341 digital polarimeter, equipped with a Toshiba sodium bulb, using a cell path length of 1 dm. Specific and molar rotation values at the sodium D line are expressed as deg dm^{-1} g^{-1} cm^3 and deg dm^{-1} mol^{-1} dL, respectively.

Circular dichroism (CD) spectra were carried out at 25 °C on $CHCl_3$ solutions on a Jasco 810 A dichrograph, using the same path lengths and solution concentrations as for the UV–vis measurements. $\Delta\varepsilon$ values, expressed as L mol^{-1} cm^{-1} were calculated from the following expression: $\Delta\varepsilon = [\Theta]/3300$, where the molar ellipticity $[\Theta]$ in deg cm^2 $dmol^{-1}$ refers to one azobenzene chromophore.

2.2. Materials

The azoic alcohol (*S*)-(−)-3-hydroxy-1-(4-azobenzene)-pyrrolidine [(*S*)-**HAP**], and the model compound (*S*)-**PAP** were synthesized as previously reported [24].

4-Dimethylaminopyridinium 4-toluenesulfonate (**DPTS**) was prepared from 4-dimethylaminopyridine and 4-toluenesulfonic acid (Aldrich) as previously described [33].

Chloroform, CCl_4, CH_2Cl_2, THF and dimethylacetamide (DMA) were purified and dried according to the reported procedures [34] and stored under nitrogen.

All other reagents and solvents were used as received.

2.3. (R)-(+)-3-Hydroxy-1-(4-azobenezene) pyrrolidine [(R)-HAP]

The previously reported procedure [24] adopted for the preparation of (*S*)-(−)-3-hydroxy-1-(4-azobenzene)pyrrolidine [(*S*)-**HAP**] was followed for the synthesis of the azoic alcohol (*R*)-(+)-3-hydroxy-1-(4-azobenzene)pyrrolidine [(*R*)-**HAP**] starting from (*R*)-(+)-malic acid instead of (*S*)-(−)-malic acid, with an overall yield of 79%, m.p. 224–226 °C.

^{1}H NMR ($CDCl_3$): 7.90 (m, 2H, arom. 2′-H), 7.85 (dd, 2H, arom. *meta* to amino group), 7.50 (m, 2H, arom. 3′-H), 7.35 (m, 1H, arom. 4′-H), 6.60 (dd, 2H, arom. *ortho* to amino group), 4.65 (m, 1H, 3-CH), 3.70–3.30 (m, 4H, 2- and 5-CH_2), 2.20 (m, 2H, 4-CH_2), 1.75 (m, 1H, OH) ppm.

FT-IR (KBr): 3414 (ν_{OH}), 3060 (ν_{CH}, arom.), 2920 and 2860 (ν_{CH}, aliph.), 1605 and 1516 ($\nu_{C=C}$ arom.), 818 (δ_{CH}, 1,4-disubst arom. ring), 763 and 689 (δ_{CH}, monosubst arom. ring) cm^{-1}.

UV–vis in THF: $\varepsilon_{max} \times 10^{-3} = 35.0$ (457 nm) and 15.8 (278 nm) L mol^{-1} cm^{-1}.

2.4. Synthesis of dimeric models

2.4.1. Separation by fractional distillation of the diastereoisomers of dimethyl-2,4-dimethylglutarate (DDMG)

Meso or *dl* enriched diastereoisomers, dimethyl-2,4-dimethylglutarate (91.1% *meso* form, ratio *meso/dl* 1/0.09) [**DDMG**-(91.1% *meso*)] (b.p. = 91.0 °C/12 mmHg) and dimethyl-2,4-dimethylglutarate (84.2% *dl* form, ratio *meso/dl* 1/5.33) [**DDMG**-(16.2% *meso*)] (b.p. = 90.0 °C/12 mmHg), were obtained by fractional distillation under reduced pressure (12 mmHg) of commercial dimethyl-2,4-dimethylglutarate (Aldrich, 58.8% *meso* form, ratio *meso/dl* 1/0.70) [**DDMG**-(58.8% *meso*)] as previously reported by Achenbach and Karl [35].

^{1}H NMR resonances used for the determination of the diastereoisomeric compositions are as follows (Fig. 4): ^{1}H NMR ($CDCl_3$): 3.70 (s, 3H, OCH_3 *dl*), 3.65 (s, 3H, OCH_3 *meso*), 2.50 (m, 2H, CH), 2.20 and 1.45 (2ddd, 2H, CH_2 *meso*), 1.75 (2 t, 2H, CH_2 *dl*), 1.20 (d, 6H, CH_3 *meso*), 1.16 (d, 6H, CH_3 *dl*) ppm.

2.4.2. 2,4-Dimethylglutaric acid (58.3% meso form) [DMG-(58.3% meso)]

An excess of KOH (171 mmol, 9.60 g, about 6 equiv. of KOH for 1 equiv. of ester) in 10 ml of water was added to a solution of commercial **DDMG-**(58.8% *meso*) (14.8 mmol, 2.79 g) in 20 ml of ethanol, and the mixture was kept under reflux, monitoring the progress of the saponification reaction by FT-IR until the disappearance of the ester absorption at 1730 cm^{-1}, completed after about 30 min. The solvent was eliminated under reduced pressure and the resulting white solid was dissolved in water. The solution was acidified (pH = 1) with concentrated aqueous HCl, and the precipitated material was filtered, dissolved in diethyl ether, dried with Na_2SO_4 and the solvent removed under vacuum to give pure 2,4-dimethylglutaric acid (58.3% *meso* form). Yield of 75%, m.p. 134–136 °C.

^{1}H NMR ($CDCl_3$): 11.2 (s, 2H, OH), 2.45 (m, 2H, CH), 2.10 and 1.45 (2ddd, 2H, CH_2 *meso*), 1.70 (2t, 2H, CH_2 *racemic*), 1.18 (d, 6H, CH_3 *meso*), 1.16 (d, 6H, CH_3 *racemic*) ppm.

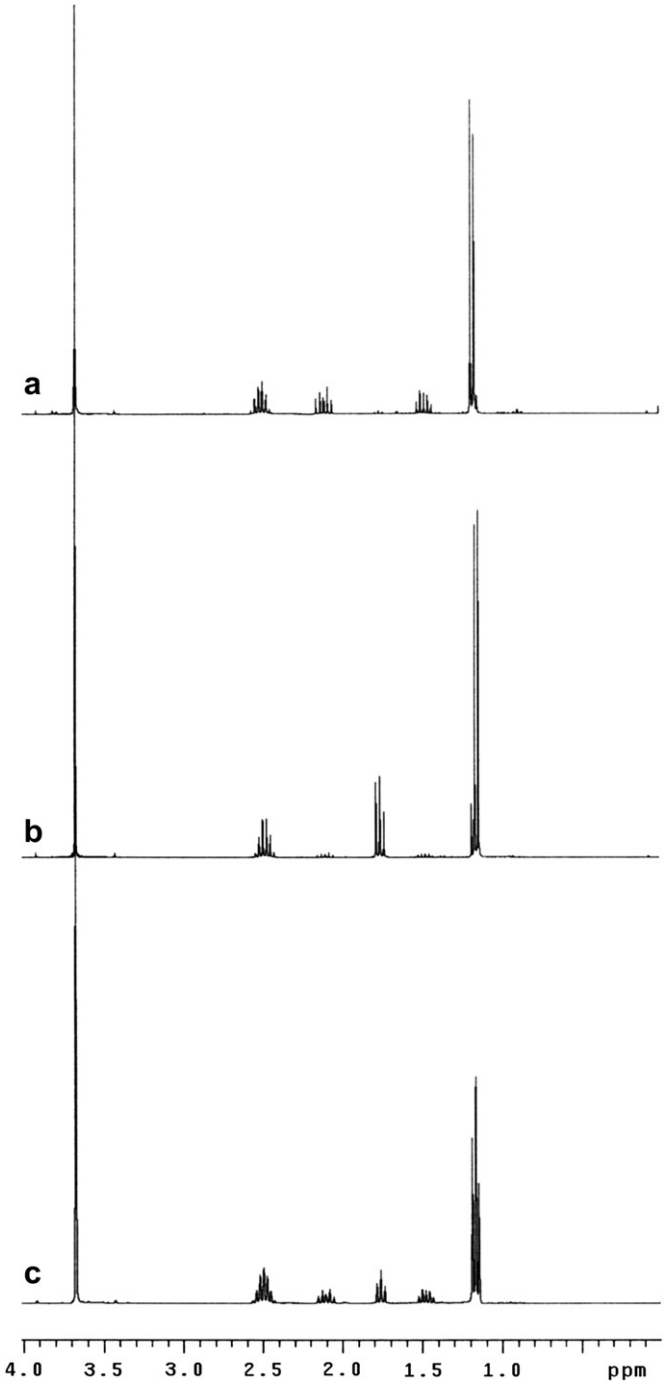

Fig. 4. ^{1}H NMR spectra in $CDCl_3$ of (a) **DDMG**-(91.1% *meso*), (b) **DDMG**-(16.2% *meso*) and (c) **DDMG**-(58.8% *meso*).

FT-IR (KBr): 3425 (ν_{OH}), 2980 (ν_{CH}), 1699 ($\nu_{C=O}$), 1457 (δ_{CHas}, CH_3), 1435 (δ_s, CH_3), 1267 (ν_{C-O}), 915 (δ_{C-O}) cm^{-1}.

*2.4.3. 2,4-Dimethylglutaric acid (90.0% meso form) [**DMG**-(90.0% meso)]*

The product was prepared by saponification of **DDMG**-(91.1% *meso*) using the same procedure described above for the diacid derivate of commercial dimethyl-2,4-dimethylglutarate. The product was obtained in 66% yield, m.p. 140–141 °C. Lit.: m.p. 142–143 °C (95% *meso* form) [35].

*2.4.4. 2,4-Dimethylglutaric acid (82.0% dl form) [**DMG**-(18.0% meso)]*

The product was prepared by saponification of **DDMG**-(16.2% *meso*) using the same procedure described above for the diacid derivate of commercial dimethyl-2,4-dimethylglutarate. The product was obtained in 71% yield, m.p. 129–130 °C. Lit.: m.p. 127–128 °C (95% *dl* form) [35].

*2.4.5. Bis{(S)-(−)-3-[1-(4-azobenzene)]pyrrolidine}-2,4-dimethylglutarate (71.0% meso form) {Dim[(S)-**DMGAP**]-(71.0% meso)}, bis{(S)-(−)-3-[1-(4-azobenzene)]pyrrolidine}-2,4-dimethylglutarate (40.9% meso form) {Dim[(S)-**DMGAP**]-(40.9% meso)}, bis{(S)-(−)-3-[1-(4-azobenzene)]pyrrolidine}-2,4-dimethylglutarate (0% meso form) {Dim[(S)-**DMGAP**]-(0% meso)} and bis{(R)-(+)-3-[1-(4-azobenzene)]pyrrolidine}-2,4-dimethylglutarate (67.6% meso form) {Dim[(R)-**DMGAP**]-(67.6% meso)}*

General procedure: 2,4-Dimethyglutaric acid (**DMG**) (1.55 mmol) and a molar excess of the azoic alcohol [(*S*)- or (*R*)-**HAP**] (6.20 mmol, 2 equiv. of alcohol for 1 equiv. of acid) were dissolved in dry CH_2Cl_2 (600 mL) under a nitrogen atmosphere. Then 4-(dimethylamino)pyridinium 4-toluenesulfonate (**DPTS**, 3.10 mmol, 1 equiv. for 1 equiv. of acid) and 1,3 diisopropylcarbodiimide (**DIPC**, 4.03 mmol, 1.3 equiv. for 1 equiv. of acid) were successively added under magnetic stirring, as condensation activator and coupling agent, respectively [27], and the mixture was kept for some days at room temperature under nitrogen flow (as reported in Table 1). The progress of the reaction was monitored by thin layer chromatography. The solid *N*,*N*-diisopropylurea, thus formed, was filtered off and the liquid phase was washed with several portions of aq 1 M HCl, aq 5% Na_2CO_3 and water, in that order. After drying the organic layer on anhydrous Na_2SO_4 and evaporation of the solvent under vacuum, the crude product was purified by column chromatography (SiO_2, $CHCl_3$/EtOAc 4:1 v/v as eluent) followed by recrystallization in *n*-pentane to afford the pure **DMGAP** derivative. Relevant data for the synthesized products are reported in Table 1.

Table 1
Relevant data for the synthesized compounds

DMG diacid	Alcohol	Dimeric model	Reaction time (days)	Yield (%)
DMG-(90.0% *meso*)	(*S*)-**HAP**	Dim[(*S*)-**DMGAP**]-(71.0% *meso*)	17	25
DMG-(58.3% *meso*)	(*S*)-**HAP**	Dim[(*S*)-**DMGAP**]-(40.9% *meso*)	5	27
DMG-(18.0% *meso*)	(*S*)-**HAP**	Dim[(*S*)-**DMGAP**]-(0% *meso*)	11	81
DMG-(90.0% *meso*)	(*R*)-**HAP**	Dim[(*R*)-**DMGAP**]-(67.6% *meso*)	13	22

FT-IR, ^{1}H and ^{13}C NMR characterization data are given below.

*2.4.5.1. Dim[(S)-**DMGAP**]-(71.0% meso) (yield 27%).* ^{1}H NMR ($CDCl_3$): 7.85 (m, 4H, arom. 2′-H), 7.80 (dd, 4H, arom. *meta* to amino group), 7.50 (m, 4H, arom. 3′-H), 7.30 (m, 2H, arom. 4′-H), 6.60 (dd, 4H, arom. *ortho* to amino group), 5.40 (m, 2H, pyrrolidine 3-CH), 3.70 and 3.40 (m, 8H, pyrrolidine 2- and 5-CH_2), 2.45 (m, 2H, backbone CH), 2.25 (m, 4H, pyrrolidine 4-CH_2), 2.10 and 1.45 (2ddd, 2H, backbone CH_2 *meso* form), 1.75 (2t, 2H, backbone CH_2 *dl* form), 1.20 (d, 6H, CH_3 *meso* form) and 1.16 (d, 6H, CH_3 *dl* form) ppm.

^{13}C NMR ($CDCl_3$): 176.3 (*C*O), 153.8, 150.1, 144.6 (arom. *C*−N═N−*C* and *C*−N−CH_2), 130.1 (arom. 4′-*C*), 129.7 (arom. 3′-*C*), 125.9, 122.9 (arom. 2′-*C* and 3-*C*), 112.3 (arom. 2-*C*), 74.3 (*C*H−O), 54.3 (CH−*C*H_2−N), 46.4 (CH_2−*C*H_2−N), 38.4 (backbone CH_2−*C*H) 38.0 (backbone *C*H_2−CH), 31.9 (*C*H_2−CH_2−N), 18.4 (backbone *C*H_3 *dl* form) and 17.8 (backbone *C*H_3 *meso* form) ppm.

FT-IR (KBr): 3069 (ν_{CH}, arom.), 2982 and 2947 (ν_{CH}, aliph.), 1734 ($\nu_{C=O}$, ester), 1605 and 1516 ($\nu_{C=C}$, arom.), 1139 (ν_{C-O}), 818 (δ_{CH}, 1,4-disubst. arom. ring), 763 and 689 (δ_{CH}, monosubst. arom. ring) cm^{-1}.

*2.4.5.2. Dim[(S)-**DMGAP**]-(0% meso) (yield 81%).* ^{1}H NMR ($CDCl_3$): 7.85 (m, 4H, arom. 2′-H), 7.80 (dd, 4H, arom. *meta* to amino group), 7.50 (m, 4H, arom. 3′-H), 7.30 (m, 2H, arom. 4′-H), 6.60 (dd, 4H, arom. *ortho* to amino group), 5.40 (m, 2H, pyrrolidine 3-CH), 3.70 and 3.40 (m, 8H, pyrrolidine 2- and 5-CH_2), 2.45 (m, 2H, backbone CH), 2.25 (m, 4H, pyrrolidine 4-CH_2), 1.75 (2 t, 2H, backbone CH_2 *dl* form) and 1.17 (d, 6H, CH_3 *dl* form) ppm.

^{13}C NMR ($CDCl_3$): 176.5 (*C*O), 153.8, 150.1, 144.6 (arom. *C*−N═N−*C* and *C*−N−CH_2), 130.1 (arom. 4′-*C*), 129.6 (arom. 3′-*C*), 125.9, 122.8 (arom. 2′-*C* and 3-*C*), 112.2 (arom. 2-*C*), 74.1 (*C*H−O), 54.3 (CH−*C*H_2−N), 46.4 (CH_2−*C*H_2−N), 38.3 (backbone CH_2−*C*H), 38.1 (backbone *C*H_2−CH), 31.9 (*C*H_2−CH_2−N) and 18.4 (backbone *C*H_3 *dl* form) ppm.

FT-IR (KBr): 3067 (ν_{CH}, arom.), 2983 and 2952 (ν_{CH}, aliph.), 1734 ($\nu_{C=O}$, ester), 1605 and 1516 ($\nu_{C=C}$, arom.), 1138 (ν_{C-O}), 818 (δ_{CH}, 1,4-disubst. arom. ring), 765 and 687 (δ_{CH}, monosubst. arom. ring) cm^{-1}.

As an example, the ^{1}H NMR spectra of dimeric models at 71% of *meso* form and 100% of *dl* form are reported in Fig. 5.

2.5. Separation of stereoisomers (SR/RS)-Dim[(S)-DMGAP]-(100% meso), (SS)-Dim[(S)-DMGAP]-(0% meso) and (RR)-Dim[(S)-DMGAP]-(0% meso)

The diastereomeric forms (*SS*)- and (*RR*)-Dim[(*S*)-**DMGAP**]-(0% *meso*) were obtained from Dim[(*S*)-**DMGAP**]-(0% *meso*) by semipreparative HPLC separation at 25 °C on a Waters HPLC Column (Nova-Pak Silica 6 μm), 7.8 × 300 mm, UV detector 254 nm, flow rate 4 mL/min (eluent THF/*n*-hexane 20:80). A sufficient amount of both the individual isomers was

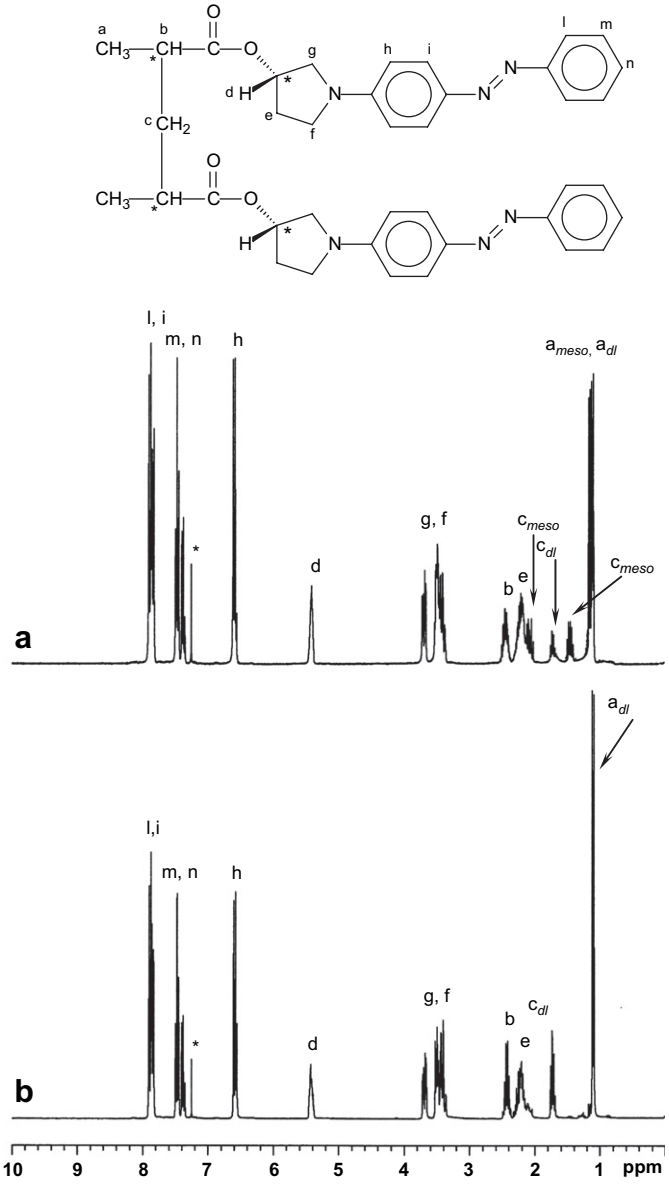

Fig. 5. ^{1}H NMR spectra in $CDCl_3$ of (a) Dim[(*S*)-**DMGAP**]-(71.0% *meso*) and (b) Dim[(*S*)-**DMGAP**]-(0% *meso*). The resonances marked with an asterisk belong to the solvent.

obtained by collecting repeated elutions of the mixture, originally composed by 29 and 71% molar contents of each form, as shown by the chromatogram reported in Fig. 6.

XRD analysis allowed us to assign the *RR* configuration to the asymmetric carbon atoms of the dimethylglutarate moiety of the predominant isomer [crystal data for (*RR*)-Dim[(*S*)-**DMGAP**]-(0% *meso*): crystal system: orthorhombic; space group: *P*2(1)2(1)2(1); $a = 10.232(2)$ Å; $b = 10.699(3)$ Å; $c = 32.075(7)$ Å; cell vol. 3511.2(13) $Å^3$; $Z = 4$; density = 1.246 g cm^{-3}; $F(000) = 1376$; $\alpha, \beta, \gamma = 90°$].

The elution by HPLC of Dim[(*S*)-**DMGAP**]-(71.0% *meso*) and -(40.9% *meso*) having a molar composition, respectively, of (*SS*)-, (*RR*)-Dim[(*S*)-**DMGAP**]-(0% *meso*) and (*SR*/*RS*)-Dim[(*S*)-**DMGAP**]-(100% *meso*) forms of 11, 18 and 71%, and 23, 38 and 39%, was carried out under the same

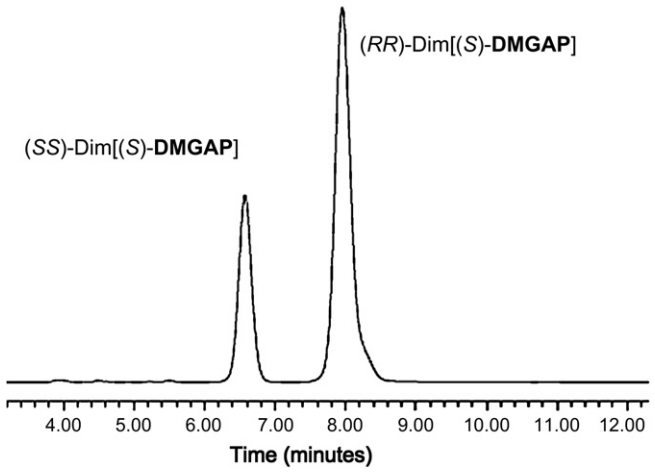

Fig. 6. HPLC chromatographic resolution of Dim[(*S*)-**DMGAP**]-(0% *meso*) in its two deastereoisomers (*SS*)- and (*RR*)-Dim[(*S*)-**DMGAP**]-(0% *meso*).

conditions as above and allowed us to obtain the pure (*SR*/*RS*)-Dim[(*S*)-**DMGAP**]-(100% *meso*) isomer (elution time 9 min).

3. Results and discussion

3.1. Synthesis and structural characterization of dimeric models

Fractional distillation under reduced pressure of commercial dimethyl-2,4-dimethylglutarate containing the 58.8% of the *meso* form [**DDMG-**(58.8% *meso*)] allowed to achieve, as previously reported by Achenbach and Karl [35], two fractions of **DDMG** containing an amount of *meso* form equal to 91.1% and 15.8% [**DDMG**-(91.1% *meso*) and **DDMG**-(15.8% *meso*)], respectively, as determined by ^{1}H NMR (Fig. 4). The two methylenic protons of glutaric moiety, in fact, result magnetically equivalent in the *dl* isomer, giving rise to a well-defined double triplet centered at about 1.75 ppm. On the other hand, the same protons are unequivalent in the *meso* isomer and appear as two double doublets of doublets centered at 2.20 and 1.45 ppm. Thus, the molar amount of *meso* and *dl* forms of 2,4-dimethylglutarate can be evaluated from the integrated values of these signals. Analogous assessment is obtained by analysis of the methyl groups resonances in the ^{13}C NMR spectra.

The above **DDMG** derivatives, as well as commercial **DDMG**, were successively hydrolyzed in the presence of an excess of KOH to the corresponding 2,4-dimethylglutaric acid (**DMG**) derivatives [35]. The reaction progress was monitored by FT-IR until disappearance of the signal at 1730 cm^{-1} related to the glutarate methyl ester. ^{1}H and ^{13}C NMR analyses confirmed that the diastereomeric composition of the diacid derivatives remains substantially analogous to that of the diester precursors, with no relevant change of composition (Scheme 1).

The diacidic **DMG** derivatives have been finally esterified to the related **DMGAP** products (Scheme 1) at room temperature, in the presence of **DIPC** and **DPTS** as coupling agent and catalyst [36], respectively, by reaction with the azoic alcohol (*R*)-**HAP**, prepared in the present work, or with its enantiomer (*S*)-**HAP**, previously reported [24].

The chemical structures of the obtained **DMGAP** products have been confirmed by FT-IR, ^{1}H and ^{13}C NMR spectra and their relevant data are reported in Table 1.

^{1}H NMR analysis (Fig. 5) allowed us to estimate the molar amounts of *meso* and *dl* forms of the dimethylglutarate residue in all the synthesized dimeric models, similarly to **DDMG** and **DMG** derivatives (Table 1). Analogous values of composition have been obtained by analysis of the methyl groups resonances in the ^{13}C NMR spectra.

As the functionalization of diacidic **DMG** with alcohol (*S*)-**HAP** gives a mixture of *meso* (*SRSS*/*SSRS*) and *dl* (*SSSS* and *SRRS*) diastereoisomers (forms **a**, **b** and **c**, respectively, in Fig. 3), semipreparative HPLC chromatography allowed us to achieve their separation with a satisfactory purity and to estimate their relative molar composition (see Section 2).

From the obtained results the following considerations can be made:

(i) The stereoisomeric composition of Dim[(*S*)-**DMGAP**]-(40.9% *meso*) resembles that usually obtained for polymethacrylic derivatives prepared by radical polymerization (30% of *isotactic* dyads in the main chain) [20,25–27,30–32], as well as for poly[(*S*)-**MAP**] (content of *isotactic* dyads about 26%) [24].

(ii) Dim[(*S*)-**DMGAP**]-(0% *meso*) constituted only by the *dl* stereoisomer, matches perfectly the *syndiotactic* dyad of poly[(*S*)-**MAP**].

(iii) Dim[(*S*)-**DMGAP**]-(71.0% *meso*) and Dim[(*R*)-**DMGAP**]-(67.6% *meso*) are composed by similar amounts of optical antipodes with opposite chirality.

(iv) the molar ratio between (*SS*)- and (*RR*)-Dim[(*S*)-**DMGAP**]-(0% *meso*) models, results approximately constant.

Also, the final compositions of the synthesized models, reported in Table 1, as well as the different reaction yields obtained, indicate that a variation of the relative amount of stereoisomers of the **DMG** residue after the functionalization of the diacids with the azoic alcohols has occurred. For instance, Dim[(*S*)-**DMGAP**]-(40.9% *meso*) is obtained by esterification of **DMG**-(58.3% *meso*), derived from commercial **DDMG**-(58.8% *meso*). Therefore, it appears that an enrichment in the *dl* component has occurred. A similar enrichment, about 17–21%, of the amount of *dl* form is also shown by other derivatives, yet with unchanged molar ratio of (*SS*) and (*RR*) diastereoisomers. In particular, Dim[(*S*)-**DMGAP**]-(0% *meso*) is obtained from **DMG**-(18.0% *meso*) almost totally as the *dl* form (Table 1).

Such a behaviour could be ascribed to the occurrence of a partial isomerization of the asymmetric carbon atoms of **DMG**, during the esterification process, however, previous data concerning the optical purity of analogous optically active products prepared through a similar synthetic pathway [31], exclude the possibility, at room temperature and in the

presence of **DIPC** and **DPTS**, of an alteration of the stereoisomeric balance as a consequence of isomerization. Another possibility could be given by different reactivity of the 2,4-dimethylglutaric acid isomers (see Fig. 2) towards the azoic alcohol, attributable to the steric hindrance of the initially produced mono-azo ester that could differently slow down the subsequent functionalization. Indeed, reaction mixtures relatively rich in the *meso* form of **DMG** give incomplete esterification of the diacid substrate, with formation of complex mixtures of several unknown products. In addition, the possibility of formation of *meso*-2,4-dimethylglutaric anhydride [36] from the *meso* diacid cannot either be excluded. As a result, the reactant *meso* substrate could display slower diesterification rate than the *dl* form, therefore leading to a significant decrease of the *meso* content in the final product.

3.2. UV–vis properties

The UV–vis spectra of chiral 2,4-dimethylglutaric derivatives (Table 2 and Fig. 7) in dilute CCl_4, $CHCl_3$, CH_2Cl_2 and DMA solutions display, in the 250–700 nm spectral region, two absorption bands centered around 403–412 and 258–260 nm. The former one, more intense, is attributed to several electronic transitions such as n–π*, π–π* and internal charge transfer of the azobenzene chromophore, the latter to the π–π* electronic transition of aromatic ring [37]. The above mentioned solvents have been selected as representatives of nonpolar, slightly polar, polar and strongly polar media, respectively.

A weak bathochromic effect (red shift) occurs for the intense first band of all samples, upon increasing solvent polarity from CCl_4 to DMA, as shown, for example, for Dim[(*S*)-**DMGAP**]-(40.9% *meso*), while the maximum absorbance wavelengths of the second band remain almost constant. This positive solvatochromism, previously reported for the model compound (*S*)-**PAP** and poly[(*S*)-**MAP**] in $CHCl_3$, THF and DMA solutions [24], is usually observed for push–pull chromophores with a neutral ground state, whose polarity increases during the electronic transition [38].

A similar, but larger, red shift was previously also observed for the 4′-nitro substituted dimeric derivative Dim[(*S*)-**DMGAP-N**]-(32.8% *meso*) (Fig. 1) (46 nm on passing from CCl_4 to DMSO) [29] with respect to those shown by the dimeric models investigated here [12 nm for Dim[(*S*)-**DMGAP**]-(40.9% *meso*) on passing from CCl_4 to DMA] (Table 2). This effect is clearly related to the variation of dipole moment induced by the increase of the electron-withdrawing character of the substituent, on passing from H to NO_2 in the 4′ position of azobenzene. As in these systems the ground state is less polar than the excited state [39], it appears that the polarity of the solvent employed favours the bathochromic shift of the absorption band.

Significant hypochromic shifts of the first band were formerly observed passing from the model (*S*)-**PAP** to the corresponding polymer poly[(*S*)-**MAP**], regardless of the solvent employed [24]. Such a behaviour, frequently noticed in several polymers bearing side chain aromatic chromophores [40–42], is attributed to the occurrence of electrostatic dipole–dipole interactions between the neighbouring aromatic chromophores [43–45].

As shown in Table 2, the molar absorption coefficients (ε_{max}) related to the first absorption band of the individual dimeric isomeric forms appear different between each other with intermediate values with respect to those observed for (*S*)-**PAP** and poly[(*S*)-**MAP**], in agreement with a reduced extent

Table 2
UV–vis spectra at 25 °C

Samples	Solvent	1st band		2nd band	
		λ_{max}[a]	$\varepsilon_{max} \times 10^{-3}$[b]	λ_{max}[a]	$\varepsilon_{max} \times 10^{-3}$[b]
Dim[(*S*)-**DMGAP**]-(71.0% meso)	$CHCl_3$	408	28.8	259	10.8
	CH_2Cl_2	410	29.6	259	10.6
Dim[(*S*)-**DMGAP**]-(40.9% meso)	CCl_4	403	25.9	n.d.	n.d.
	$CHCl_3$	408	28.7	259	10.9
	CH_2Cl_2	410	30.4	259	11.0
	DMA	412	29.0	260	11.6
Dim[(*S*)-**DMGAP**]-(0% meso)	$CHCl_3$	407	30.4	259	10.7
	CH_2Cl_2	410	31.1	259	10.4
Dim[(*R*)-**DMGAP**]-(67.6% meso)	$CHCl_3$	408	28.8	259	10.9
	CH_2Cl_2	410	29.5	259	10.8
(*SR/RS*)-Dim[(S)-**DMGAP**]-(100% meso)	$CHCl_3$	408	29.4	259	10.9
(*SS*)-Dim[(*S*)-**DMGAP**]-(0% meso)	$CHCl_3$	409	28.5	258	10.8
(*RR*)-Dim[(*S*)-**DMGAP**]-(0% meso)	$CHCl_3$	408	29.4	258	10.9
(*S*)-**PAP**	$CHCl_3$[c]	409	29.8	258	11.6
	CH_2Cl_2	412	31.4	258	10.6
	DMA[c]	416	29.5	258	11.7
Poly[(*S*)-**MAP**]	$CHCl_3$[c]	408	28.3	258	10.5
	CH_2Cl_2	411	29.4	259	10.8
	DMA[c]	413	29.1	260	10.7

[a] Wavelength of maximum absorbance, expressed in nm.
[b] Expressed in L mol^{-1} cm^{-1} and calculated for one single chromophore.
[c] See Ref. [24].

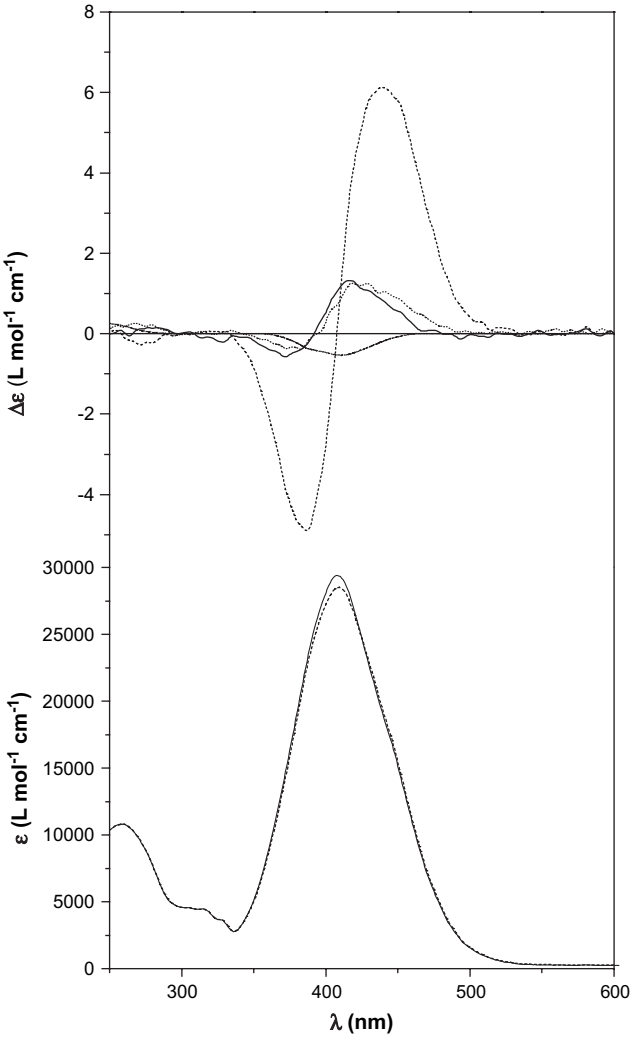

Fig. 7. (Bottom) UV–vis spectra in chloroform solution of (*SS*)- (---) and (*RR*)-Dim[(*S*)-**DMGAP**]-(0% *meso*) (—); (up) CD spectra in chloroform solution of (*SS*)- (---), (*RR*)-Dim[(*S*)-**DMGAP**]-(0% *meso*) (—), (*SR*/*RS*)-Dim[(*S*)-**DMGAP**]-(100% *meso*) (···) and model compound (*S*)-**PAP** (-••-).

of intramolecular interactions between chromophores as compared to the polymeric derivative. However, no clear behaviour related to the configuration of the stereomeric centers of the DMG residue is observed, the conformational arrangement of the chromophores in solution resulting probably the dominating factor affecting the absorption coefficient value.

3.3. Optical activity, CD spectra and chiroptical properties

The specific $[\alpha]_D^{25}$ and molar $[\Phi]_D^{25}$ optical rotations of the synthesized dimeric derivatives have been determined in $CHCl_3$ solution at the sodium D line and compared with the values obtained by the model compound (*S*)-**PAP** and the corresponding homopolymeric poly[(*S*)-**MAP**] (Table 3).

The reaction of optically inactive diacid **DMG** with the chiral alcohol (*S*)-**HAP** gives a mixture of *meso* and *dl* diastereoisomers **a** (*SRSS* ≡ *SSRS*), **b** (*SSSS*) and **c** (*SRRS*); the same reaction with (*R*)-**HAP**, instead, gives the diastereoisomers

Table 3
Specific and molar optical rotation data of dimeric derivatives in $CHCl_3$ solution

Samples	$[\alpha]_D^{25}$[a]	$[\Phi]_D^{25}$[b]
(*SR*/*RS*)-Dim[(*S*)-**DMGAP**]-(100% *meso*)	+40	+134
(*SS*)-Dim[(*S*)-**DMGAP**]-(0% *meso*)	+355	+1191
(*RR*)-Dim[(*S*)-**DMGAP**]-(0% *meso*)	+6	+20
Dim[(*S*)-**DMGAP**]-(71.0% *meso*)	+69	+232
Dim[(*S*)-**DMGAP**]-(40.9% *meso*)	+101	+340
Dim[(*S*)-**DMGAP**]-(0% *meso*)	+124	+415
Dim[(*R*)-**DMGAP**]-(67.6% *meso*)	−75	−252
(*S*)-**PAP**[c]	+4.0	+14.0
Poly[(*S*)-**MAP**][c]	+410.0	+1374.0

[a] Specific optical rotation, expressed as deg dm^{-1} g^{-1} dL ($c \approx 0.250$ g/dL).
[b] Molar optical rotation, expressed as deg dm^{-1} mol^{-1} dL and calculated as ($[\alpha]_D^{25}M/100$), where *M* represents the molecular weight of (*S*)-**PAP** or the molecular weight of the repeating unit of poly[(*S*)-**MAP**] or the half molecular weight of the dimers; in other word, the molar optical rotation calculated for chromophoric unit.
[c] See Ref. [24].

d (*RRSR* ≡ *RSRR*), **e** (*RRRR*) and **f** (*RSSR*) (Fig. 3). The individual diastereoisomers **a**, **b** and **c** (Fig. 3), separated by HPLC, show specific optical rotation values very different from each other (Table 3); isomer **b** (*SSSS*) displays a $[\alpha]_D^{25}$ value surprisingly high (+355 deg dm^{-1} g^{-1} dL), much higher than those of **a** (*SRSS*/*SSRS*) and **c** (*SRRS*) (+40 and +6, respectively). Such a behaviour could be due to a different conformational arrangement of the chromophores with respect to the main chain plane, as represented in Fig. 2 for the *syndiotactic* and *isotactic* dyads, and these results indicate that the optical activity of these derivatives may depend on the chiral interactions between a couple of chromophores only: indeed, the monomeric model (*S*)-**PAP**, containing only one chromophoric unit, displays negligible optical activity, as reported in Table 3.

The optical activity of all the dimeric mixtures results strictly related to the % amount of each form. Being the acidic precursors *meso* and *dl* **DMG** optically inactive [35], the measured $[\alpha]_D^{25}$ values of the azoaromatic derivatives reported in Table 3, are to be attributed to the presence in the molecule of the two pyrrolidine chiral centers with the same absolute configuration.

Increasing the % of the *meso* form of **DMG** residue (from 0 to 71.0%), the amount of stereoisomer **b** ($[\alpha]_D^{25} = +355$) in the mixture is progressively reduced and the overall optical activity decreases. The experimental values of specific optical rotation are consistent with the diastereomeric compositions determined by chromatographic separation, thus excluding any influence on optical activity by intermolecular interactions in solution between different diastereomeric forms. In fact, Dim[(*S*)-**DMGAP**]-(0% *meso*), 100% of *dl* form of the **DMG** residue, constituted by 71% of stereoisomer **c** ($[\alpha]_D^{25} = +6$) and 29% of **b** ($[\alpha]_D^{25} = +355$), displays $[\alpha]_D^{25} = +124$.

Considering now that the stereoisomer pairs **a** *vs.* **d** and **b**–**c** *vs.* **e**–**f** are optical antipodes (Fig. 3), Dim[(*R*)-**DMGAP**] (67.6% *meso*), constituted by **d**–**e**–**f** diastereoisomers show, as expected, optical activity very close and with opposite

sign of Dim[(*S*)-**DMGAP**] (71.0% *meso*) ($[\alpha]_D^{25} = -75$ and +69, respectively).

On the basis of the above determined values of +355 and +6 for the *dl* (*SS*) and (*RR*) diastereoisomers, respectively, and +40 for the *meso* model compound, poly[(*S*)-**MAP**], which is constituted by 74 and 26% of syndio (*dl*) and isotactic (*meso*) dyads [24], should display a specific optical activity similar to that one of Dim[(*S*)-**DMGAP**]-(40.9% *meso*) (around +100), much lower than the value of +410.0, experimentally found (Table 3).

This finding thus suggests that a substantial contribution to the overall optical activity of poly[(*S*)-**MAP**], is given by the presence of longer sequences of optically active co-units, as previously observed for oligomeric poly[(*S*)-**MAP**] derivatives [28].

To evidence the presence of conformationally ordered *trans*-azobenzenic chromophores, the dimeric model compounds have been investigated by CD in chloroform solution in the spectral region between 250 and 700 nm (Table 4, Figs. 7 and 8).

In contrast with the monomeric model (*S*)-**PAP** [24], displaying weak negative and positive signals centered at about 410 and 258 nm, respectively (Table 4 and Fig. 7), related to the first and second UV–vis absorptions, the CD spectra of all the samples synthesized here show, in the spectral region connected to the first UV–vis band, two dichroic bands of opposite sign and slightly different intensity (Table 4, Figs. 7 and 8), with cross-over points close to their UV–vis maximum absorptions (Table 2).

Such a behaviour is indicative of exciton splitting determined by cooperative dipolar interactions between the neighbouring optically active azoaromatic chromophores [46–48] disposed in a mutual chiral geometry of one prevailing handedness [24,26–29].

The presence of exciton couplets points out that the interchromophoric interactions, responsible for the intensity and the shape of the dichroic bands, are similar in the model dyads to those occurring in the related poly[(*S*)-**MAP**] [24]. As shown in Fig. 7, the different intensity of the CD absorptions displayed by the three diastereoisomers **a**, **b** and **c**, appears

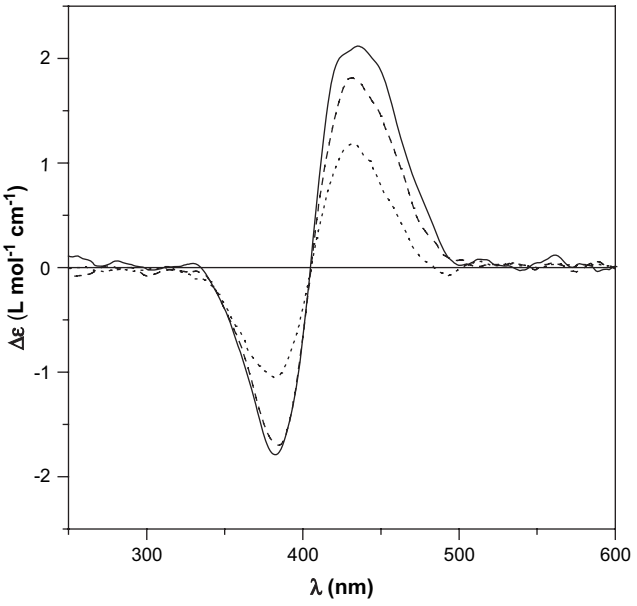

Fig. 8. CD spectra in chloroform solution of Dim[(*S*)-**DMGAP**]-(0% *meso*) (—), Dim[(*S*)-**DMGAP**]-(40.9% *meso*) (---), Dim[(*S*)-**DMGAP**]-(71.0% *meso*) (···).

strongly dependent on the absolute configuration of the two chiral carbons of the DMG residues, and in agreement with the results obtained by polarimetry (Table 3): stereoisomer **b** displays, in correspondence to the first UV–vis absorption band, an intense excitonic couplet; in contrast, **a** and **c** show spectra with the same shape but of reduced intensity.

As a consequence, the CD spectra of Dim[(*S*)-**DMGAP**]-(71.0% *meso*), Dim[(*S*)-**DMGAP**]-(40.9% *meso*) and Dim[(*S*)-**DMGAP**]-(0% *meso*) result strongly dependent on their diastereoisomeric composition (Table 4 and Fig. 8). Indeed, by increasing the amount of *dl* compounds (in particular of **b**) (Fig. 3), model of the *syndiotactic* dyad of poly[(*S*)-**MAP**], a progressive enhancement of dichroic bands intensity and therefore of the overall optical activity is observed.

In this context, and in agreement with polarimetric data (Table 3), the integrated area of the dichroic bands connected

Table 4
CD spectra in $CHCl_3$ solution at 25 °C

Samples	1st absorption band					2nd absorption band	
	λ_1[a]	$\Delta\varepsilon_1$[b]	λ_0[c]	λ_2[a]	$\Delta\varepsilon_2$[b]	λ_3[a]	$\Delta\varepsilon_3$[b]
(*S*)-**PAP**[d]	410	−0.51	–	–	–	258	+0.22
(*SR*/*RS*)-Dim[(*S*)-**DMGAP**]-(100% *meso*)	423	+1.25	397	380	−0.37	n.d.[e]	n.d.[e]
(*SS*)-Dim[(*S*)-**DMGAP**]-(0% *meso*)	440	+6.07	408	386	−4.90	271	−0.31
(*RR*)-Dim[(*S*)-**DMGAP**]-(0% *meso*)	415	+1.24	393	372	−0.67	n.d.[e]	n.d.[e]
Dim[(*S*)-**DMGAP**]-(71.0% *meso*)	430	+1.11	404	382	−1.08	n.d.[e]	n.d.[e]
Dim[(*S*)-**DMGAP**]-(40.9% *meso*)	431	+1.98	405	385	−1.99	n.d.[e]	n.d.[e]
Dim[(*S*)-**DMGAP**]-(0% *meso*)	432	+2.31	405	382	−1.98	n.d.[e]	n.d.[e]
Dim[(*R*)-**DMGAP**]-(67.6% *meso*)	431	−1.10	405	383	+1.12	n.d.[e]	n.d.[e]
Poly[(*S*)-**MAP**][d]	445	+7.35	409	387	−6.42	258	−0.32

[a] Wavelength of maximum dichroic absorption, expressed in nm.
[b] $\Delta\varepsilon$ expressed in ($L\,mol^{-1}\,cm^{-1}$) and calculated for chromophoric unit.
[c] Wavelength of the cross-over of dichroic bands, expressed in nm.
[d] See Ref. [24].
[e] Not determinable due to low intensity of the signals.

to the first UV–vis absorption band, measured for Dim[(*S*)-**DMGAP**]-(40.9% *meso*) is about one fourth of the related band area measured for poly[(*S*)-**MAP**].

Recently, we have established that the positive Cotton effect observed in the CD spectra of the dimeric model compound Dim[(*S*)-**DMGAP-N**]-(32.8% *meso*) is related to a right-handed chiral conformation of the azoaromatic chromophores [29]. The observation of Cotton effects with the same sign for the dimers reported in Figs. 7 and 8 would therefore indicate a right-handed helix sense of the conformational arrangement of the azobenzenic moieties. In this context, the CD spectra of Dim[(*S*)-**DMGAP**]-(71.0% *meso*) and Dim[(*R*)-**DMGAP**]-(67.9% *meso*) (Table 4 and Fig. 9) are, as indicated by polarimetric data, the mirror image of each other, thus indicating an opposite conformational screw sense of the chromophores in these samples.

Such a behaviour is due to the functionalization of the **DMG** residue with the azoic alcohol (*S*)-**HAP** or its enantiomer (*R*)-**HAP** which gives rise to a mixture of **a**–**b**–**c** and **d**–**e**–**f** stereoisomers (optical antipods having similar optical activity but opposite sign, as represented in Fig. 3), respectively, as discussed above.

It can be therefore concluded that the presence of pyrrolidine moieties of different absolute configurations (*S* or *R*) in the side chain is fundamental to originate a well-determined helix-sense of neighbouring chromophores.

This behaviour confirms that the CD signals exhibited by this class of optically active polymers may be attributed to the presence of relatively short chain segments with a well-defined prevailing helical conformation strongly depending on chain length, as previously shown for some methacrylic oligomers [28] and polymers with different average polymerization degrees (in the range 10–30) [26–28].

To better clarify this point and to further explore how the macromolecular tacticity affects the optical activity it would be, however, necessary to prepare and investigate fully *isotactic* and *syndiotactic* polymers and the related oligomers as models of stereoregular triads, tetrads, etc.

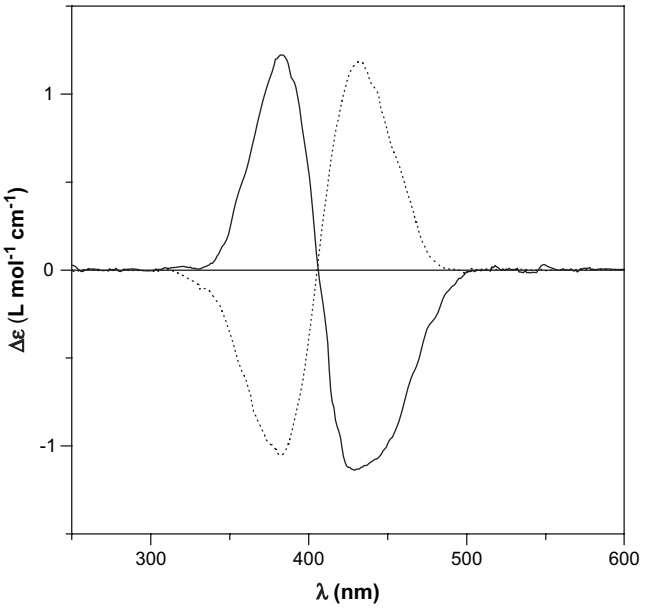

Fig. 9. CD spectra in chloroform solution of Dim[(*R*)-**DMGAP**]-(67.6% *meso*) (—) and Dim[(*S*)-**DMGAP**]-(71.0% *meso*) (···).

4. Conclusions

Well-defined new optically active *meso* and *dl* compounds containing the optically active residue of 3-(*S*)-pyrrolidine have been synthesized by functionalization of 2,4-dimethylglutaric acid as dimeric models for *isotactic* and *syndiotactic* dyads of the related photochromic methacrylic polymers containing azoaromatic moieties in the side chain. By HPLC we have been able to separate the three diastereoisomeric compounds (*SS*)-, (*RR*)-Dim[**DMGAP**]-(0% *meso*) and (*RS*/*SR*)-Dim[**DMGAP**]-(100% *meso*). All the obtained compounds have been fully characterized with the aim to establish the effects of diastereoisomeric composition on their optical activity and to correlate the (micro)tacticity to the chiroptical properties of the corresponding polymeric materials.

In agreement with the results obtained by polarimetry, the CD spectra of the dimeric models display approximately the same shape as the related polymer, but with reduced intensity.

CD spectra and optical rotation values shown by the pair Dim[(*S*)-**DMGAP**]-(71.0% *meso*) and Dim[(*R*)-**DMGAP**]-(67.9% *meso*) confirm that the chiroptical properties of the related macromolecules are connected to the configurations (*S*) and (*R*), respectively, of the side chain of optically active azoaromatic pyrrolidine moiety, which determines the conformational screw sense assumed by the dimers and by chain sections with one prevailing helical conformation of the correspondent methacrylic macromolecular main chain.

On the basis of the chirooptical properties shown by the three diastereoisomeric models, poly[(*S*)-**MAP**], which is constituted by 74 and 26% of syndio (*dl*) and isotactic (*meso*) dyads, respectively [24], should display an overall chirality much lower than that experimentally found. This confirms that although an important contribution to optical activity is given by the prevalent (micro)tacticity of the polymeric backbone, the prevailing chirality of the macromolecules is determined by the conformational arrangement of the azoaromatic chromophores.

Acknowledgements

The financial support by MIUR and Consortium INSTM (FIRB2001 'RBNE01P4JF') is gratefully acknowledged.

References

[1] Green MM, Nolte RJM, Meijer EW, Denmark SE, Siegel J. Topics in stereochemistry: materials-chirality, vol. 24. New York: Wiley-VCH; 2003.
[2] Zhang J, Albelda Mt, Liu Y, Canary JW. Chirality 2005;17:404–20.
[3] Kajitani T, Okoshi K, Sakurai S, Kumaki J, Yashima E. J Am Chem Soc 2006;128:708–9.
[4] Yashima E, Maeda K, Nishimura T. Chem Eur J 2004;10:42–51.
[5] Wilson AJ, Masuda M, Sijbesma RP, Meijer EW. Angew Chem Int Ed 2005;44:2275–9.

[6] Green MM, Park J-W, Sato T, Teramoto A, Lifson S, Selinger RLB, et al. Angew Chem Int Ed 1999;38:3138.
[7] Farina M. The stereochemistry of linear macromolecules. In: Topics in stereochemistry, vol. 17. New York: Wiley-Inter-science; 1987. p. 1–111.
[8] Green MM, Peterson NC, Sato T, Teramoto A, Cooks RG, Lifson S. Science 1995;268:1860.
[9] Mayer S, Maxein G, Zentel R. Macromol Symp 1999:137.
[10] Li J, Schuster GB, Cheon K-S, Green MM, Selinger JV. J Am Chem Soc 2000;122:2603.
[11] Maxein G, Zentel R. Macromolecules 1995;28:8438;
Műller M, Zentel R. Macromolecules 1996;29:1609.
[12] Carlini C, Angiolini L, Caretti D. Photochromic optically active polymers. In: Polymeric materials encyclopaedia, vol. 7. Boca Raton: CRC Press; 1996. p. 5116.
[13] Proceedings of the symposium on azobenzene-containing materials, Boston MA (USA) 1998. In: Natansohn A, editor. Macromol Symp 1999; 137:1–165.
[14] Verbiest T, Kauranen M, Persoons A. J Mater Chem 1999;9:2005.
[15] Delaire JA, Nakatani K. Chem Rev 2000;100:1817–46.
[16] Hopkins TE, Wagener KB. Adv Mater 2002;14:1703.
[17] Xie S, Natansohn A, Rochon P. Chem Mater 1995;5:403.
[18] Todorov T, Nikolova L, Tomova N. Appl Opt 1984;23:4588–91.
[19] Andruzzi L, Altomare A, Ciardelli F, Solaro R, Hvilsted S, Ramanujam PS. Macromolecules 1999;32:448–54.
[20] Angiolini L, Benelli T, Bozio R, Daurù A, Giorgini L, Pedron D, et al. Macromolecules 2006;39:489.
[21] Angiolini L, Bozio R, Daurù A, Giorgini L, Pedron D, Turco G. Chem—Eur J 2002;8:4241.
[22] Angiolini L, Benelli T, Bozio R, Daurù A, Giorgini L, Pedron D. Synth Met 2003;139:743.
[23] Angiolini L, Bozio R, Giorgini L, Pedron D. Synth Met 2003;138:375.
[24] Angiolini L, Caretti D, Giorgini L, Salatelli E. J Polym Sci Part A Polym Chem 1999;37:3257.
[25] Angiolini L, Caretti D, Giorgini L, Salatelli E. Polymer 2001;42:4005.
[26] Angiolini L, Benelli T, Giorgini L, Salatelli E. Polymer 2005;46:2424.
[27] Angiolini L, Benelli T, Giorgini L, Salatelli E. Macromolecules 2006; 39:3731–7.
[28] Angiolini L, Benelli T, Giorgini L, Salatelli E. Polymer 2006;47: 1875–85.
[29] Painelli A, Terenziani F, Angiolini L, Benelli T, Giorgini L. Chem—Eur J 2005;11:6053.
[30] McCord E, Anton WL, Wilczek L, Ittel SD, Nelson LTJ, Raffell KD. Macromol Symp 1994;86:47.
[31] Angiolini L, Caretti D, Giorgini L, Salatelli E, Altomare A, Carlini C, et al. Polymer 1998;39:6621.
[32] Peat IR, Reynolds WF. Tetrahedron Lett 1972:1359.
[33] Moore JS, Stupp S. Macromolecules 1990;23:65.
[34] Perrin DD, Amarego WLF, Perrin DR. Purification of laboratory chemicals. Oxford: Pergamon Press; 1966.
[35] Achenbach H, Karl W. Chem Ber 1975;108:759.
[36] Bartlett PA, Richardson DP, Myerson J. Tetrahedron 1984;40:2317.
[37] Altomare A, Ciardelli F, Ghiloni MS, Solaro R, Tirelli N. Macromol Chem Phys 1997;198:1739.
[38] Reichardt C. Chem Rev 1994;94:2319.
[39] Hallas G. J Soc Dyers Colour 1979;95:285.
[40] Chiellini E, Solaro R, Galli G, Ledwith A. Macromolecules 1980;13: 1654.
[41] Majumdar RN, Carlini C. Makromol Chem 1980;181:201.
[42] Carlini C, Gurzoni F. Polymer 1983;24:101.
[43] Tinoco Jr I. J Am Chem Soc 1960;82:4785.
[44] Okamoto K, Itaya A, Kusabayashi S. Chem Lett 1974:1167.
[45] Ciardelli F, Aglietto M, Carlini C, Chiellini E, Solaro R. Pure Appl Chem 1982;54:521.
[46] Rodger A, Nordén B. Circular dichroism, and linear dichroism. Oxford: Oxford University Press; 1997 [chapters 5 and 7].
[47] Mason SF. Molecular optical activity and the chiral discrimination. Cambridge: Cambridge University Press; 1982 [chapter 3].
[48] Berova N, Nakanishi K, Woody RW. Circular dichroism, principles and applications. New York: Wiley-VCH; 2000.